Nonlinear magnetic susceptibility and aging phenomena in a reentrant ferromagnet: $Cu_{0.2}Co_{0.8}Cl_2$-$FeCl_3$ graphite bi-intercalation compound

Masatsugu Suzuki* and Itsuko S. Suzuki†
Department of Physics, State University of New York at Binghamton, Binghamton, New York 13902-6000, USA
(Received 28 July 2003; revised manuscript received 24 November 2003; published 23 April 2004)

Linear and nonlinear dynamic properties of a reentrant ferromagnet $Cu_{0.2}Co_{0.8}Cl_2$-$FeCl_3$ graphite bi-intercalation compound are studied using ac and dc magnetic susceptibility. This compound undergoes successive phase transitions at the transition temperatures $T_h(=16\ \mathrm{K})$, $T_c(=9.7\ \mathrm{K})$, and $T_{RSG}(=3.5\ \mathrm{K})$. The static and dynamic behaviors of the reentrant spin-glass phase below T_{RSG} are characterized by those of normal spin-glass phase with critical exponent $\beta=0.57\pm0.10$ and a dynamic critical exponent $x=8.5\pm1.8$. In the ferromagnetic phase $(T_{RSG}\leqslant T\leqslant T_c)$, a prominent nonlinear magnetic susceptibility is observed. The relaxation of the absorption $\chi''(\omega,t)$ with time t exhibits a weak power-law decay: $\chi''(\omega,t)\approx t^{-b''}$ where $b''\approx0.07$. These results suggest a chaotic nature of ferromagnetic phase.

DOI: 10.1103/PhysRevB.69.144424 PACS number(s): 75.40.Gb, 75.50.Lk, 75.30.Kz, 75.70.Cn

I. INTRODUCTION

The nature of a reentrant spin-glass (RSG) phase and a ferromagnetic (FM) phase in reentrant ferromagnets has been a topic of much controversy.[1–15] Spin frustration effects occur as a result of a competition between ferromagnetic interactions as a majority and antiferromagnetic interactions as a minority. As the temperature is lowered, the reentrant ferromagnet exhibits first a transition from a paramagnetic (PM) phase to a FM phase with decreasing temperature and then a second transition from the FM phase to a RSG phase. Such a reentry behavior of the reentrant ferromagnets has been extensively studied experimentally in the last two decades.[1–15] There are four types of reentrant ferromagnets: (i) metallic spin glasses such as $Fe_{0.7}Al_{0.3}$,[1,2] $(Fe_{0.20}Ni_{0.80})_{75}P_{16}B_6Al_3$,[3–5] $(Fe_{1-x}Mn_x)_{75}P_{16}B_6Al_3$ $(0.2\leqslant x\leqslant0.32)$,[6] and $N_{77}Mn_{22}$ (Refs. 7 and 8) having Ruderman-Kittel-Kasuya-Yosida- type interactions between distant spins, (ii) insulating spin glasses such as $CdCr_{2x}In_{2(1-x)}S_4$ $(0.90\leqslant x<1)$,[9–12] (iii) dilute magnetic semiconductors such as $Eu_xSr_{1-x}S$ $(0.52\leqslant x\leqslant0.60)$,[13,14] and (iv) colossal magnetoresistance materials such as $Y_{0.7}Ca_{0.3}MnO_3$.[15] In the case of (ii) and (iii), ferromagnetic nearest-neighbor interactions compete with antiferromagnetic next-nearest-neighbor interactions.

The nature of the RSG and FM phases in reentrant ferromagnets is basically understood in terms of a mean-field picture. The phase diagram (T/J vs J_0/J) of the Sherrington-Kirkpatrick (SK) model with Ising spins[16] consists of the PM phase, FM phase, and the spin-glass (SG) phase, where an infinite-ranged Gaussian distribution of exchange interactions with variance J and mean J_0 is assumed.[17] For $J_0/J\leqslant1$, as T is lowered, the system undergoes a transition from the PM phase to the SG phase. For $J_0/J>1$, as T is lowered, the system undergoes a PM-FM transition followed by a FM-SG transition. This SG phase for $J_0/J>1$ is called a RSG phase. However, the nature of the RSG phase is essentially the same as that of the normal SG phase for $J_0/J\leqslant1$. When the Parisi's solution for the SK model[18,19] is discovered, the vertical phase boundary at $J_0/J=1$ is added to the SK phase diagram. For $J_0/J>1$, consequently the whole RSG phase and a part of the FM phase in the SK model are newly replaced by a RSG phase with replica symmetry breaking (RSB). This RSG phase is very different from the normal SG phase for $J_0/J\leqslant1$. It is a mixed phase of the normal SG phase and the FM phase.

In the mean-field picture, a reentrance from the FM phase to the normal SG phase is predicted. There is a normal FM long-range order in the FM phase. This picture, which assumes infinite-range interactions, is not always appropriate for real reentrant magnets where the short-range interactions are large and random in sign and the spin symmetry is rather Heisenberg-like than Ising-like. Neutron-scattering studies on $(Fe_{1-x}Mn_x)_{75}P_{16}B_6Al_3$ (Ref. 6) have questioned the existence of a true long-range order even in the FM phase. Aeppli *et al.*[6] have proposed a phenomenological random-field picture to explain their result. In this picture, the system in the FM phase consists of regions which would order ferromagnetically and other regions forming PM clusters. The frustrated spins in the PM clusters can generate random molecular fields, which act on the unfrustrated spins in the infinite FM network. In the FM phase well above T_{RSG}, the fluctuations of the spins in the PM clusters are so rapid that the FM network is less influenced by them and their effect is only to reduce the net FM moment. On decreasing the temperature toward T_{RSG}, the thermal fluctuations of the spins in the PM clusters become slower. The coupling between the PM clusters and the FM network becomes important and the molecular field from the slow PM spins acts as a random magnetic field. This causes breakups of the FM network into finite-sized clusters. Below T_{RSG}, the ferromagnetism completely disappears, leading to a SG phase. This picture is very different from the mean-field picture. The RSG phase is not a mixed phase but a normal SG phase.

Jonason *et al.*[4,5] have shown from a dynamic scaling analysis of low-field dynamic susceptibility of $(Fe_{0.20}Ni_{0.80})_{75}P_{16}B_6Al_3$ that there is a spin-glass relaxation time which diverges at a finite temperature with a dynamic critical exponent similar to that observed for an ordinary PM-SG transition. This suggests that the RSG phase is a

normal SG phase. The FM phase just above T_{RSG} shows a dynamic behavior characterized by an aging effect and chaotic nature similar to that of SG phase. Dupuis *et al.*[12] have shown that the aging behavior of the low-frequency ac susceptibility is observed both in the FM phase and RSG phase of $CdCr_{2x}In_{2(1-x)}S_4$ with $x=0.90$, 0.95, and 1.00, with the same qualitative features as in normal spin glasses. It seems that these results are explained in terms of the random-field picture.

In this paper we report our experimental study on the magnetic properties of the RSG phase and the FM phase of a reentrant ferromagnet $Cu_{0.2}Co_{0.8}Cl_2$-$FeCl_3$ graphite bi-intercalation compound (GBIC). This compound undergoes three phase transitions at $T_h(=16\ \mathrm{K})$, $T_c(=9.7\ \mathrm{K})$, and $T_{RSG}(=3.5\ \mathrm{K})$. There are the helical spin ordered phase between T_h and T_c, the FM phase between T_c and T_{RSG}, and the RSG phase below T_{RSG}.[20–22] The static and dynamic natures of the FM and RSG phases are examined from the linear and nonlinear ac magnetic susceptibilities, and the zero-field cooled (ZFC) and field-cooled (FC) magnetization. The time dependence of the ac susceptibility, showing the aging phenomena, is also studied. The nature of the RSG phase of $Cu_{0.2}Co_{0.8}Cl_2$-$FeCl_3$ GBIC is discussed in comparison with that of the SG phase of $Cu_{0.5}Co_{0.5}Cl_2$-$FeCl_3$ GBIC.[23,24] Note that $Cu_{0.5}Co_{0.5}Cl_2$-$FeCl_3$ GBIC magnetically behaves like an ideal three-dimensional (3D) short-range SG and undergoes a SG phase transition at $T_{SG}=3.92\pm0.11$ K. The dynamic scaling analysis suggests that the SG phase does not survive in the presence of H (at least above 100 Oe).[23]

$Cu_{0.2}Co_{0.8}Cl_2$-$FeCl_3$ GBIC has a unique layered structure where the $Cu_{0.2}Co_{0.8}Cl_2$ intercalate layer ($=I_1$) and $FeCl_3$ intercalate layers ($=I_2$) alternate with a single graphite layer (G), forming a stacking sequence ($\text{-}G\text{-}I_1\text{-}G\text{-}I_2\text{-}G\text{-}I_1\text{-}G\text{-}I_2\text{-}G\text{-}\cdots$) along the c axis. In the $Cu_{0.2}Co_{0.8}Cl_2$ intercalate layer two kinds of magnetic ions (Cu^{2+} and Co^{2+}) are randomly distributed on the triangular lattice. The spin order in the $Cu_{0.2}Co_{0.8}Cl_2$ layers is coupled with that in the $FeCl_3$ intercalate layer ($=I_2$) through an interplanar exchange interaction, leading to the spin frustration effect.

II. EXPERIMENTAL PROCEDURE

A sample of stage-2 $Cu_{0.2}Co_{0.8}Cl_2$ graphite intercalation compound (GIC) as a starting material was prepared from single-crystal kish graphite (SCKG) by vapor reaction of anhydrated $Cu_{0.2}Co_{0.8}Cl_2$ in a chlorine atmosphere with a gas pressure of $\approx$740 Torr.[20–23] The reaction was continued at 500 °C for three weeks. The sample of $Cu_{0.2}Co_{0.8}Cl_2$-$FeCl_3$ GBIC was prepared by a sequential intercalation method: the intercalant $FeCl_3$ was intercalated into empty graphite galleries of stage-2 $Cu_{0.2}Co_{0.8}Cl_2$ GIC. A mixture of well-defined stage-2 $Cu_{0.2}Co_{0.8}Cl_2$ GIC based on SCKG and single-crystal $FeCl_3$ was sealed in vacuum inside Pyrex glass tubing, and was kept at 330 °C for two weeks. The stoichiometry of the sample is represented by $C_m(Cu_{0.2}Co_{0.8}Cl_2)_{1-x}(FeCl_3)_x$. The concentration of C and Fe (m and x) was determined from weight uptake measurement and electron microprobe measurement [using a scanning electron microscope (Model Hitachi S-450)]: $m=7.54\pm0.05$ and $x=0.56\pm0.02$. The $(00L)$ x-ray-diffraction measurements of stage-2 $Cu_{0.2}Co_{0.8}Cl_2$ GIC and $Cu_{0.2}Co_{0.8}Cl_2$-$FeCl_3$ GBIC were made at 300 K by using a Huber double-circle diffractometer with a Mo$K\alpha$ x-ray radiation source (1.5 kW). The c-axis repeat distance of stage-2 $Cu_{0.2}Co_{0.8}Cl_2$ GIC and $Cu_{0.2}Co_{0.8}Cl_2$-$FeCl_3$ GBIC was determined as 12.81 ± 0.04 and 18.79 ± 0.05 Å, respectively.

The dc magnetization and ac susceptibility were measured using a superconducting quantum interference device magnetometer (Quantum Design, MPMS XL-5) with an ultra-low-field capability option. First a remnant magnetic field was reduced to zero field (exactly less than 3 mOe) at 298 K for both dc magnetization and ac susceptibility measurements. Then the sample was cooled from 298 to 1.9 K in a zero field.

(i) *Measurements of the zero-field-cooled susceptibility* (χ_{ZFC}) *and the field-cooled susceptibility* (χ_{FC}): After an external magnetic field H ($0\leqslant H\leqslant 5$ kOe) was applied along the c plane (basal plane of graphene layer) at 1.9 K, χ_{ZFC} was measured with increasing temperature (T) from 1.9 to 20 K. After annealing of sample for 10 min at 100 K in the presence of H, χ_{FC} was measured with decreasing T from 20 to 1.9 K.

(ii) *ac susceptibility measurement*: The frequency (f), magnetic field, and temperature dependence of the dispersion (Θ_1'/h) and absorption (Θ_1''/h) were measured between 1.9 and 20 K, where the frequency of the ac field is $f=0.01$–1000 Hz and the amplitude h is typically $h=1$ mOe–4.2 Oe.

III. RESULT

A. Nonlinear ac susceptibility: Θ_1'/h and Θ_1''/h

We have measured the dispersion Θ_1'/h and absorption Θ_1''/h at fixed T as a function of h, where 1 mOe$\leqslant h\leqslant$4.2 Oe and $f=1$ Hz. Both Θ_1'/h and Θ_1''/h are strongly dependent on h, suggesting the existence of nonlinear magnetic susceptibility. We determine the T dependence of nonlinear ac magnetic susceptibilities (χ_3', χ_5', χ_3'', χ_5'') from the least-squares fits of the data to the power-law forms:[25]

$$\Theta_1'/h=\chi_1'+3\chi_3'h^2/4+10\chi_5'h^4/16+\cdots \tag{1}$$

and

$$\Theta_1''/h=\chi_1''+3\chi_3''h^2/4+10\chi_5''h^4/16+\cdots. \tag{2}$$

Note that for convenience we use the linear ac susceptibility χ' and χ'' instead of χ_1' and χ_1''. In Figs. 1(a) and 1(b) we show the T dependence of the dispersion Θ_1'/h and the absorption Θ_1''/h at $f=1$ Hz. The different curves correspond to different amplitudes of the ac field, where h is varied between 1 mOe and 4.2 Oe. The susceptibilities Θ_1'/h and Θ_1''/h are independent of h for $h<h_0$ within experimental error, where $h_0\approx0.1$ Oe, implying that Θ_1'/h and Θ_1''/h coincide with the linear susceptibilities χ' and χ'', respectively. Note that Θ_1''/h shows a sharp peak at 4 K, which is almost

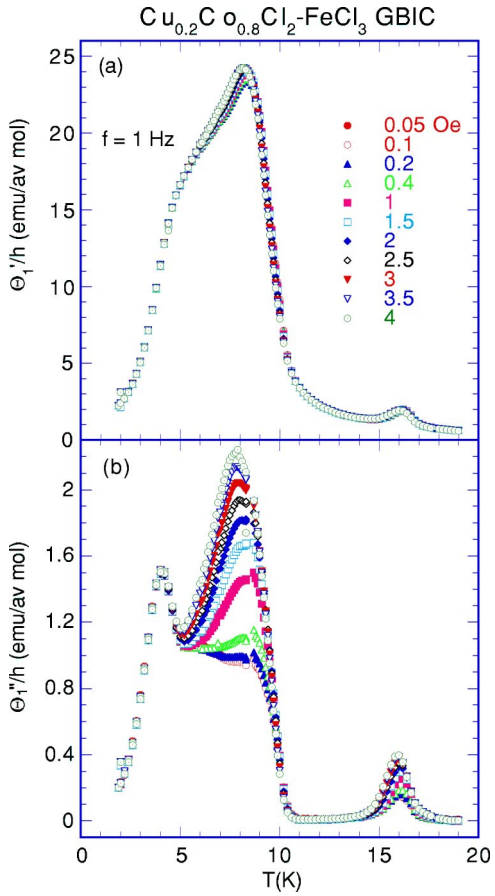

FIG. 1. (Color online) T dependence of (a) Θ_1'/h and (b) Θ_1''/h at various h for $Cu_{0.2}Co_{0.8}Cl_2$-$FeCl_3$ GBIC. $h\perp c$, $f=1$ Hz, $H=0$.

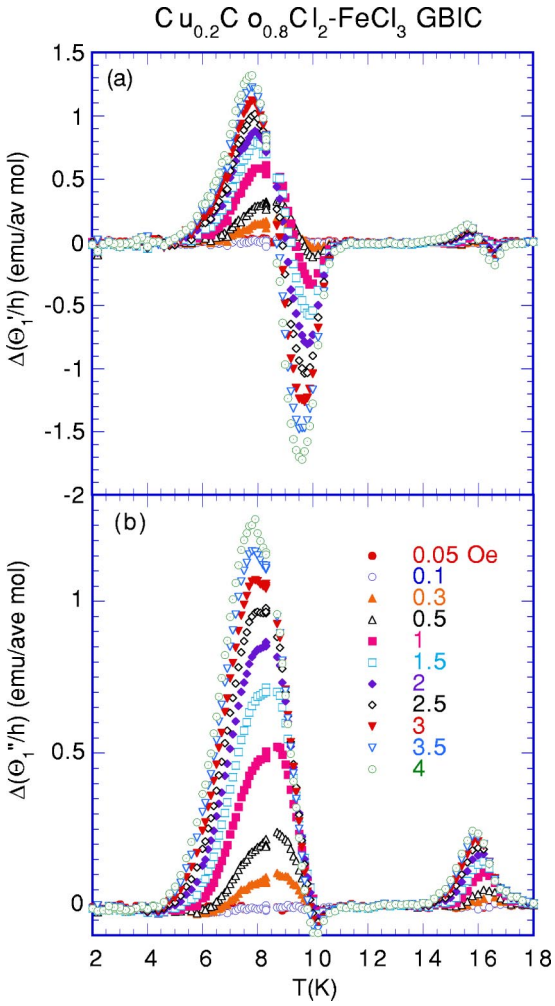

FIG. 2. (Color online) T dependence of (a) $\Delta(\Theta_1'/h)$ and (b) $\Delta(\Theta_1''/h)$ at various h. $f=1$ Hz, $H=0$. $\Delta(\Theta_1'/h)$ is defined by the difference between Θ_1'/h at h ($h>30$ mOe) and Θ_1'/h at $h=30$ mOe. $\Delta(\Theta_1''/h)$ is defined by the difference between Θ_1''/h at h ($h>30$ mOe) and Θ_1''/h at $h=30$ mOe.

independent of h. This sharp peak is associated with the transition between the FM and RSG phases: $T_{RSG}=3.5$ K.

In Figs. 2(a) and 2(b) we show the T dependence of $\Delta(\Theta_1'/h)$ and $\Delta(\Theta_1''/h)$ at various h, where $\Delta(\Theta_1'/h)$ and $\Delta(\Theta_1''/h)$ are defined as the differences between Θ_1'/h and Θ_1''/h at h ($h>30$ mOe) and those at $h=30$ mOe, respectively: $\Delta(\Theta_1'/h)=3\chi_3'h^2/4+10\chi_5'h^4/16+\cdots$ and $\Delta(\Theta_1''/h)=3\chi_3''h^2/4+10\chi_5''h^4/16+\cdots$. The differences $\Delta(\Theta_1'/h)$ and $\Delta(\Theta_1''/h)$ are strongly dependent on h. The difference $\Delta(\Theta_1''/h)$ has two local maxima at 16.2 K (15.8 K) and 8.6 K (7.8 K), and a local minimum at 10.3 K (10.1 K) at $h=1$ Oe ($h=4$ Oe). In contrast, $\Delta(\Theta_1'/h)$ has two local maxima at 15.8 K (15.6 K) and 8.3 K (7.8 K), and two local minima at 9.9 K (9.5 K) and 16.6 K (16.5 K) at $h=1$ Oe ($h=4$ Oe). In summary, the positions of the local maxima and minima shift to low-T side as h increases.

In Figs. 3(a) and 3(b) we show the plot of $\Delta(\Theta_1''/h)$ and $\Delta(\Theta_1'/h)$ as a function of h^2 near T_c ($=9.7$ K), respectively. Both $\Delta(\Theta_1''/h)$ and $\Delta(\Theta_1'/h)$ are strongly dependent on h^2 in these limited temperature regions. A linear increase of $\Delta(\Theta_1'/h)$ and $\Delta(\Theta_1''/h)$ with h^2 at low h indicates a positive sign of χ_3' and χ_3''. We find a peak in $\Delta(\Theta_1'/h)$ $[\Delta(\Theta_1''/h)]$ at a peak field h_p' $[h_p'']$, which shifts to the low-h side with increasing T. The fields h_p' and h_p'' are defined as $d(\Theta_1'/h)/dh=0$ and $d(\Theta_1''/h)/dh=0$, respectively: $h_p'^2\approx -3\chi_3'/(5\chi_5')$ and $h_p''^2\approx -3\chi_3''/(5\chi_5'')$. The existence of h_p' and h_p'' indicates a negative sign of χ_5' and χ_5''. In the inset of Fig. 3(a), we show the T dependence of h_p' and h_p''. The peak fields h_p' and h_p'', which decrease with increasing T, tend to reduce to zero around 9.8 and 10.4 K, respectively.

The least-squares fits of the data (Θ_1'/h vs h^2 and Θ_1''/h vs h^2) at each T for 30 mOe $\leqslant h \leqslant 0.7$ Oe to Eqs. (1) and (2) yield the values of χ_1', χ_3', χ_5', . . . and χ_1'', χ_3'', χ_5'', ... Figure 4 shows the T dependence of χ_3', χ_5', χ_3'', and χ_5'' thus obtained. The nonlinear susceptibility χ_3' at $f=1$ Hz shows a positive peak at 16.0 K, a negative local minimum at 10.2 K, and two positive peaks at 8.8 and 8.3 K. The sign of χ_3' changes from negative to positive at 9.65 K and from positive to negative at 4.0 K with decreasing T. No anomaly is observed below 4 K. In contrast, χ_5' at $f=1$ Hz exhibits a negative local minimum at 16.0 K, a positive peak at 10.2 K, and two negative peaks at 9.0 K and 8.3 K. The sign of χ_5' changes from negative to positive at 4.0 K with decreasing T.

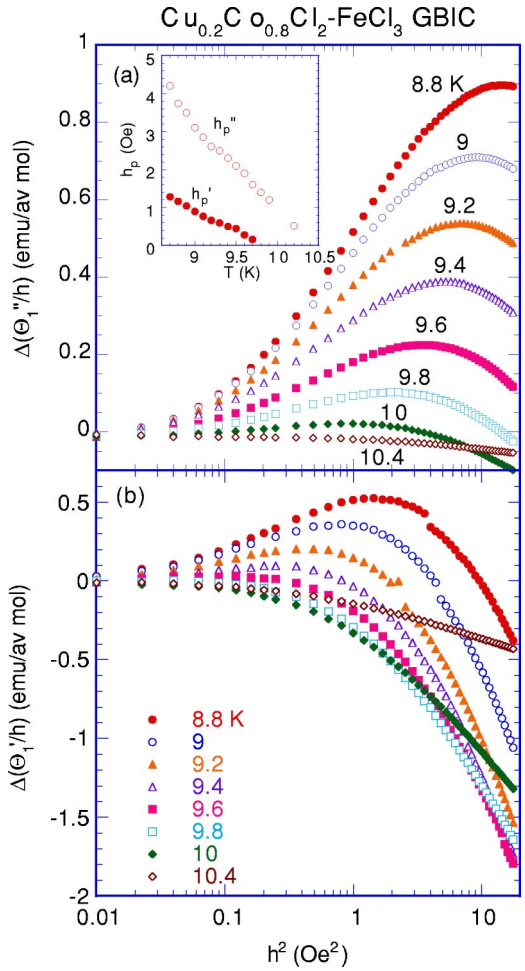

FIG. 3. (Color online) (a) and (b) h^2 dependence of $\Delta(\Theta_1''/h)$ and $\Delta(\Theta_1'/h)$ at various T. $f=1$ Hz. The inset of (a) shows the T dependence of the peak field h_p' for $\Delta(\Theta_1'/h)$ and h_p'' for $\Delta(\Theta_1''/h)$.

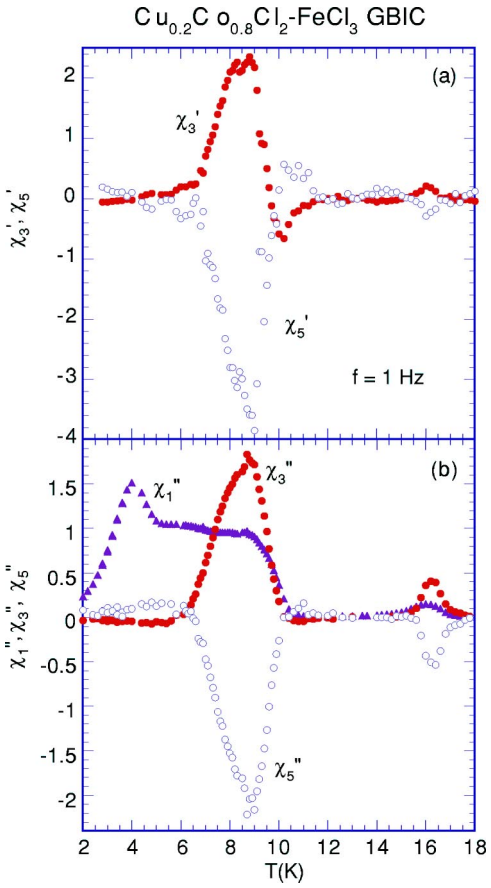

FIG. 4. (Color online) (a) T dependence of χ_3' and χ_5', where the units of χ_{2n+1}' are emu/(av mol Oe^{2n+1}). $f=1$ Hz. (b) T dependence of χ_1'', χ_3'', and χ_5'', where the units of χ_{2n+1}'' are emu/(av mol Oe^{2n+1}).

We note that the T dependence of χ_3' around 10 K in our system is similar to that in stage-2 $CoCl_2$ GIC which magnetically behaves like a quasi-2D ferromagnet with an extremely weak antiferromagnetic interplanar exchange interaction.[25] In stage-2 $CoCl_2$ GIC, χ_3' exhibits a negative local minimum at 10.5 K, becomes positive below 10.2 K, and shows a positive peak below the upper critical temperature T_{cu}.

The nonlinear susceptibility χ_3'' shows a positive peak at 16.2 K, a negative local minimum at 11.0 K, and a positive peak at 8.7 K. The sign of χ_3'' changes from negative to positive at 9.9 K and from positive to negative at 5.7 K with decreasing T. In contrast, χ_5'' shows a negative local minimum at 16.4 K, a positive peak at 11.0 K, and a negative peak at 9.0 K. The sign of χ_5'' changes from negative to positive at 6.5 K with decreasing T.

Here we discuss the T dependence of χ_3'. Basically the singularity of χ_3' could reflect the breaking of spatial magnetic symmetry. The sign of χ_3' is negative for the PM phase and the SG phase and positive for the FM phase. Thus the critical temperatures T_c for the helical spin order to FM transition and T_{RSG} for the FM-RSG transition could be defined as temperatures at which the sign of χ_3' changes. Using this definition, in fact we find 9.65 K as T_c and 4.0 K as T_{RSG} at $f=1$ Hz for our system. Similar behaviors have been reported in other reentrant ferromagnets. Sato and Miyako[26] have reported that the sign of χ_3' in $(Pd_{0.9966}Fe_{0.0034})_{0.95}Mn_{0.05}$ changes from negative to positive at T_c. Sato *et al.*[7] have shown that the sign of χ_3' in $Ni_{77}^{57}Fe_1Mn_{22}$ changes from positive to negative at T_{RSG}: χ_3' has a small negative local minimum near T_{RSG}.

B. Linear ac susceptibility: χ' and χ''

Figures 5(a) and 5(b) show the T dependence of the linear ac susceptibilities χ' and χ'' below 12 K at $h=50$ mOe, where $\Theta_1'/h=\chi_1'=\chi'$ and $\Theta_1''/h=\chi_1''=\chi''$. The absorption χ'' at $f=0.01$ Hz shows a relatively sharp peak at 3.69 K. This peak shifts to the high-T side with increasing f: 5.10 K at $f=1$ kHz. In contrast, the derivative $d\chi''/dT$ at $f=0.01$ Hz shows two negative local minima at 4.0 K corresponding to T_{RSG} and 10.0 K corresponding to T_c. The local minimum $d\chi''/dT$ vs T at 4.0 K shifts to the high-T side with increasing f, while the local minimum at 10.0 K does not shift with increasing f.

Figures 5(c) and 5(d) show the T dependence of χ' and χ'' around T_h at $h=500$ mOe, where $\Theta_1'/h \approx \chi'$ and Θ_1''/h

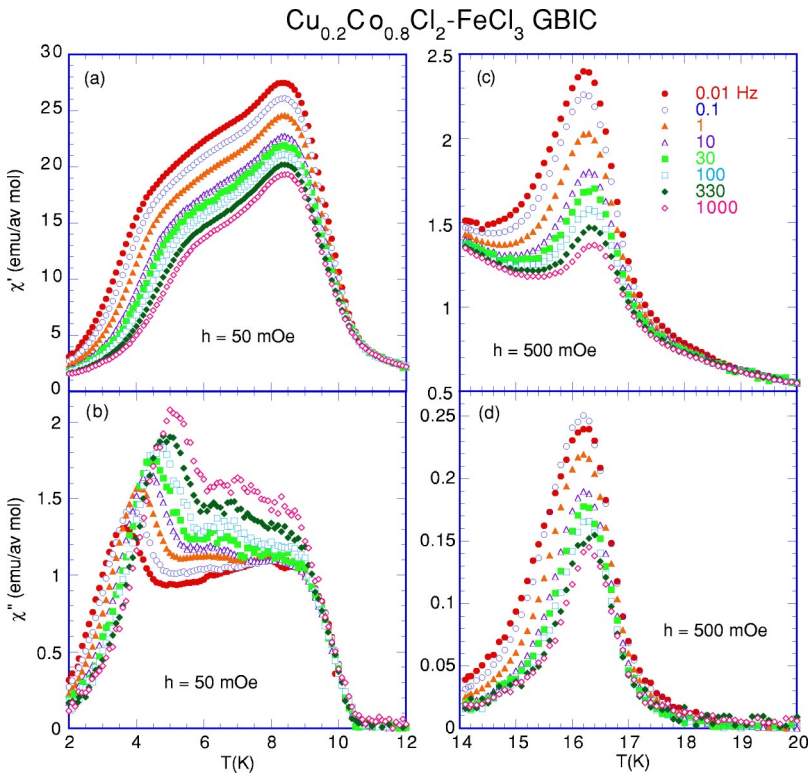

FIG. 5. (Color online) (a,b) T dependence of $\chi'(=\chi_1')$ and $\chi''(=\chi_1'')$ at various f. $h=50$ mOe, $H=0$, $2\leqslant T\leqslant 12$ K. (c,d) T dependence of $\chi'(\approx\chi_1')$ and $\chi''(\approx\chi_1'')$ at various f. $h=500$ mOe, $H=0$, $14\leqslant T\leqslant 20$ K.

$\approx\chi''$. The dispersion χ' at $f=0.01$ Hz shows peaks at 16.2 K and 8.35 K. The peak at 16.2 K slightly shifts to the high-T side with increasing f: 16.4 K at $f=1$ kHz. Another peak at 8.35 K does not shift with increasing f. The dispersion χ' at $f=0.01$ Hz has an inflection point at 3.5 K corresponding to the positive peak of $d\chi'/dT$, and another inflection point at 9.7 K corresponding to the negative local minimum of $d\chi'/dT$. The inflection point at 3.5 K shifts to the high-T side with increasing f.

Here we assume that the singular behavior of χ'' around 4 K is due to the critical slowing down associated with the FM-RSG transition. Either the peak temperatures of χ'' vs T and $T\chi''$ vs T or the local-minimum temperature of $d\chi''/dT$ vs T around 4 K coincide with a spin freezing temperature T_f, at a relaxation time $\tau\,(\approx 1/\omega)$. The relaxation time τ can be described by[27]

$$\tau=\tau^*(T_f/T_{RSG}-1)^{-x}, \tag{3}$$

where $x=\nu z$, z is the dynamic critical exponent, ν is the critical exponent of the spin-correlation length ξ, and τ^* is the characteristic time. In Fig. 6 we show the T dependence of τ thus obtained for $d\chi''/dT$. The least-squares fits of the data of τ vs T yield $x=8.5\pm 1.8$, $T_{RSG}=3.45\pm 0.31$ K, and $\tau^*=(4.77\pm 0.10)\times 10^{-6}$sec for the local-minimum temperature of $d\chi''/dT$ vs T. Note that the same method ($d\chi''/dT$ vs T) was used to determine τ vs T for the SG phase transition of $Cu_{0.5}Co_{0.5}Cl_2$-$FeCl_3$ GBIC.[23] The value of x is on the same order as that ($x=7.9$) reported by Jonason *et al.*[4] for the FM-RSG transition of $(Fe_{0.20}Ni_{0.80})_{75}P_{16}B_6Al_3$. A relatively good agreement between the value of x for $Cu_{0.2}Co_{0.8}Cl_2$-$FeCl_3$ GBIC and the value predicted by Ogielski[28] for the 3D $\pm J$ Ising SG ($x=7.9\pm 1.0$) suggests that the FM-RSG transition in our system is dynamically similar to an ordinary PM-SG transition. Note that the value of τ^* for $d\chi''/dT$ vs T is much larger than a typical value of microscopic relaxation time τ_0 (typically 10^{-10}–10^{-12}sec). Such a large value of τ^* has been also reported by Kleemann *et al.*[29] for $Co_{80}Fe_{20}/Al_2O_3$ multilayers: $\tau^*=(6.7\pm 0.4)\times 10^{-7}$sec and $x=10.0\pm 3.6$. The large τ^* suggests that the PM clusters play a significant role in the FM-RSG transition. In the random-field picture,[6] the FM phase consists of the FM region with a longer relaxation time and the PM clusters with a shorter relaxation time. On decreasing T toward

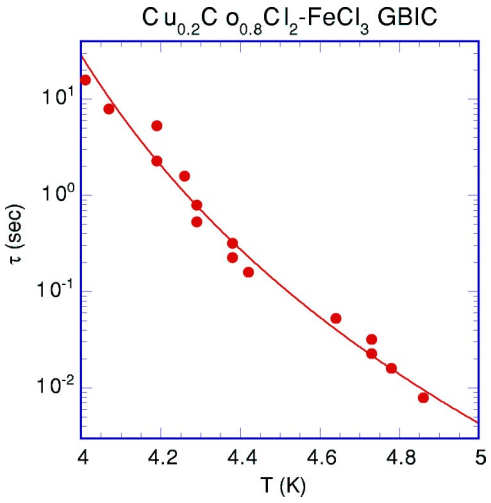

FIG. 6. (Color online) T dependence of the relaxation time τ which is determined from the f dependence of peak temperature of $d\chi''/dT$ vs T. The solid line denotes the least-squares fit of the data to Eq. (3).

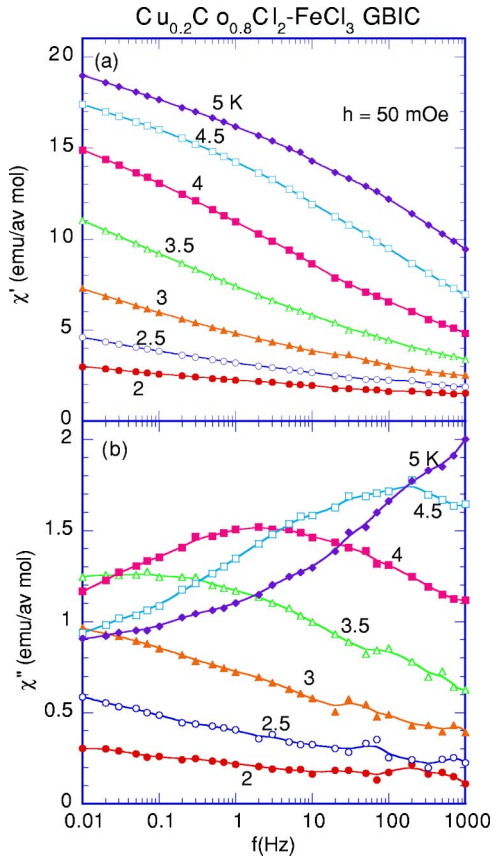

FIG. 7. (Color online) f dependence of (a) χ' and (b) χ'' at various T. $h=50$ mOe.

T_{RSG}, the thermal fluctuations of the spins in the PM clusters become slower. The molecular field of the slow PM spins acting as random magnetic field causes breakups of the FM network into finite-sized clusters. It is predicted that the following dynamic scaling equation is valid for the normal SG phase:[30] $T\chi''=\omega^{y}\Omega(\omega\tau)$, where $\Omega(\omega\tau)$ is a scaling function of $\omega\tau$ and is assumed to take a maximum at $\omega\tau=$const. The value $y(=\beta/x)$ is a critical exponent, where β is a critical exponent of the order parameter. The curve of $T\chi''$ vs T exhibits a peak, which shifts to the high-T side as f increases. The peak height of $T\chi''$ increases with increasing f. The least-squares fit of the data for the peak height of $T\chi''$ vs f (for $0.01\leqslant f\leqslant 1000$ Hz) to the form of $(\approx\omega^{y})$ yields $y=0.066\pm0.001$. Then the value of $\beta(=xy)$ is estimated as $\beta=0.57\pm0.10$, where $x=8.5\pm1.8$. This value of β is similar to that ($\beta=0.54$) for $Fe_{0.5}Mn_{0.5}TiO_3$.[31]

Figures 7(a) and 7(b) show the f dependence of $\chi'(T,\omega)$ and $\chi''(T,\omega)$ at various T in the vicinity of T_{RSG}, respectively. The absorption $\chi''(T,\omega)$ curves exhibits different characteristics depending on T. Above T_{RSG}, $\chi''(T,\omega)$ shows a peak at a characteristic frequency, shifting to the low-f side as T decreases. Below T_{RSG}, $\chi''(T,\omega)$ shows no peak for $f\geqslant0.01$ Hz. It decreases with increasing f, following a power-law form $(\approx\omega^{-\alpha''})$. This is in contrast to the f dependence of χ'' for conventional spin-glass systems such as $Fe_{0.5}Mn_{0.5}TiO_3$: χ'' increases with increasing f.[27] The exponent α'' is weakly dependent on T: $\alpha''=0.083\pm0.004$ at 2.5 K and $\alpha''=0.079\pm0.002$ at 3 K. According to the fluctuation-dissipation theorem, the magnetic fluctuation spectrum $P(\omega)$ is related to $\chi''(T,\omega)$ by $P(T,\omega)=2k_BT\chi''(T,\omega)/\omega$. Then $P(T,\omega)$ is proportional to $\omega^{-1-\alpha''}$, which is similar to $1/\omega$ character of typical spin glass. In contrast, $\chi'(T,\omega)$ decreases with increasing f above and below T_{RSG}: χ' exhibits a power-law form $(\omega^{-\alpha'})$. The exponent α' is weakly dependent on T: $\alpha'=0.079\pm0.001$ at $T=2.5$ K and $\alpha'=0.094\pm0.001$ at $T=3.0$ K. The value of α' is on the same order as that of α''. Note that χ'' is related to χ' through a so-called "$\pi/2$ rule": $\chi''=-(\pi/2)d\chi'/d\ln\omega$ (Kramers-Kronig relation), leading to the relation $\alpha'=\alpha''$.

Here we note the f dependence of χ'' above 5 K [which is not shown in Fig. 7(b)]. The absorption χ'' increases with increasing f for $5\leqslant T\leqslant7.2$ K. A newly small peak is added around $f=2$ Hz for $7.3\leqslant T\leqslant9.2$ K. The absorption χ'' decreases with increasing f for $f\leqslant70$ Hz and increases with further increasing f for $9.3\leqslant T\leqslant9.8$ K. Above 9.9 K it decreases with increasing f. We find that χ'' for $6.1\leqslant T\leqslant7.3$ K can be described by a power-law form $(\approx\omega^{\beta''})$ in the limited frequency range $(0.01\leqslant f<10$ Hz). The exponent β'' increases with increasing T: $\beta''=0.04\pm0.01$ at 6.1 K, 0.081 ± 0.02 at 6.7 K, and 0.12 ± 0.01 at 7.2 K.

C. χ_{FC}, χ_{ZFC}, and $\delta\chi(=\chi_{FC}-\chi_{ZFC})$

Figure 8 shows the T dependence of χ_{FC} and χ_{ZFC} at various H, where H is applied along the c plane which is perpendicular to the c axis. It is strongly dependent on H. The susceptibility χ_{FC} at $H=0.5$ Oe decreases with increasing T. It has inflection points at $T=16.4$, 9.70, and 4.0 K where $d\chi_{FC}/dT$ exhibits negative local minima. These temperatures correspond to the transition temperatures T_h, T_c, and T_{RSG}. In contrast, χ_{ZFC} at $H=0.5$ Oe exhibits two peaks at 16.2 and 8.2 K, and an inflection point at 3.2 K where $d\chi_{ZFC}/dT$ shows a positive local maximum. The peaks of χ_{ZFC} at 8.2 and 16.2 K shift to the low-T side with increasing H. The deviation of χ_{ZFC} at $H=0.5$ Oe from χ_{FC} starts to occur at temperatures above 18 K. The peak of χ_{ZFC} at T_h is very sensitive to the application of H. It shifts to the low-T side with increasing H and disappears above 50 Oe.

Figure 9 shows the T dependence of the difference $\delta\chi$ $(=\chi_{FC}-\chi_{ZFC})$ at various H. The difference $\delta\chi$ has three inflection points at T_h, T_c, and T_{RSG}, where $d(\delta\chi)/dT$ exhibits negative local minima: 16.2 K $(\approx T_h)$, 9.60 K $(\approx T_c)$, and 3.40 K $(\approx T_{RSG})$. The T dependence of $\delta\chi$ shown in Fig. 9 is similar to standard one observed in many reentrant ferromagnets, where $\delta\chi$ is strongly dependent on H and remains finite up to T_c at low enough fields. Typical examples of χ_{ZFC} vs T and χ_{FC} vs T have been reported for $CdCr_{2x}In_{2(1-x)}S_4$,[12] $Au_{85}Fe_{15}$,[32] $Ni_{77}Mn_{23}$,[33] and $(Fe_{0.90}Cr_{0.05}Ni_{0.05})_2P$.[34] In our system both inflection points of $\delta\chi$ at $T_c(H)$ and $T_h(H)$ become less pronounced with increasing H. Only an inflection point at $T_{RSG}(H)$ survives for $H\geqslant100$ Oe. Note that the inflection point at $T_{RSG}(H)$

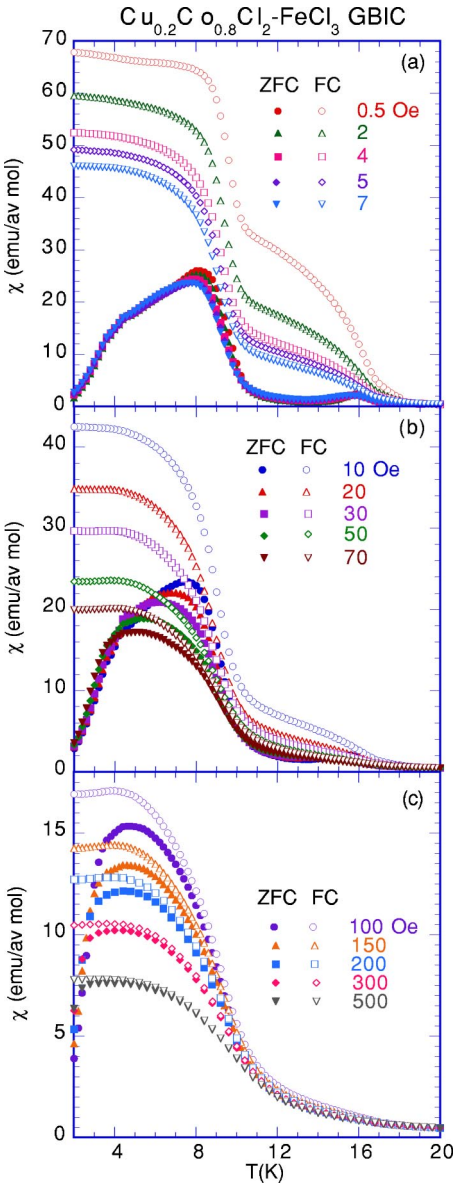

FIG. 8. (Color online) (a–c) T dependence of χ_{ZFC} and χ_{FC} at various H. $H \perp c$.

shifts to the low-T side with increasing H:2.8 K at $H=100$ Oe. The H dependence of $T_{RSG}(H)$ will be discussed in Sec. III D.

D. H-T phase diagram

We have measured the T dependence of χ' and χ'' at various H for $f=100$ Hz and 0.1 Hz, where H ($0<H \leqslant 2$ kOe) is applied along the c plane perpendicular to the c axis. Figure 10 shows the T dependence of χ' and χ'' at various H for $f=100$ Hz. The ac field $h(=50$ mOe) was used for $1.9 \leqslant T \leqslant 12$ K and a larger $h(=500$ mOe) was used for $14 \leqslant T \leqslant 19$ K. The peak of χ' and the shoulder of χ'' around T_c disappear for $H \geqslant 50$ Oe, and the peaks of χ' and χ'' around T_h disappear for $H \geqslant 7$ Oe. The peak of χ'' around T_{RSG} shifts to the low-T side with increasing H for $0 \leqslant H \leqslant 1$ kOe. The peak of χ'' around T_h also shifts to the low-T

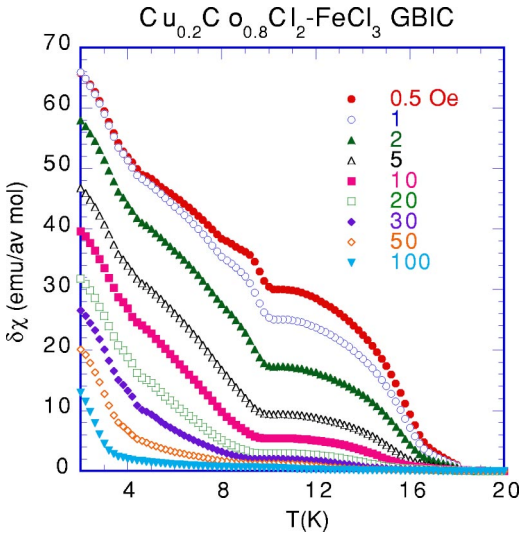

FIG. 9. (Color online) T dependence of $\delta\chi(=\chi_{FC}-\chi_{ZFC})$ at various H. The value of $\delta\chi$ is derived from Fig. 8.

side with increasing H for $0 \leqslant H \leqslant 7$ Oe. In Fig. 11 we show the line $T_f(H)$ around T_{RSG} in the H-T diagram, where the local-minimum temperature of $d\delta\chi/dT$ vs T is plotted as a function of H. The least-squares fit of the data of the line $T_f(H)$ (the local-minimum temperature of $d\delta\chi/dT$ vs T) for $0 \leqslant H \leqslant 100$ Oe to

$$H = H_0^*[1 - T_f(H)/T_g^*]^p \tag{4}$$

yields parameters $p=1.43\pm0.20$, $T_g^*=3.59\pm0.13$ K, and $H_0^*=(0.90\pm0.31)$ kOe. The exponent $p(=1.43)$ is on the same order as that $(=1.52\pm0.10)$ for $Cu_{0.5}Co_{0.5}Cl_2$-$FeCl_3$ GBIC,[23] which was also determined from the data of the line $T_f(H)$ (the local-minimum temperature of $d\delta\chi/dT$ vs T).

For comparison, the peak temperatures of $\chi''(T,H,\omega)$ vs T at $f=0.1$ Hz are also plotted as a function of H in Fig. 11. The data are well fitted to Eq. (4) with $p=1.72\pm0.10$, $T_g^*=3.82\pm0.06$ K, and $H_0^*=(2.58\pm0.60)$ kOe.

E. $\chi''(t,\omega)$ and $\chi'(t,\omega)$

In order to reveal a possible aging phenomenon in the FM phase, we have measured the t dependence of χ'' and χ' at $T=7$ and 8.5 K, where $H=0$. The system was quenched from 100 K to T at time (age) zero. Both χ' and χ'' were measured simultaneously as a function of time t at constant T. Each point consists in the successive measurements at various frequencies ($0.05 \leqslant f \leqslant 1$ Hz). Figure 12 shows the t dependence of χ'' and χ' at $T=7$ K for $f=0.05$ and 1 Hz, respectively. The absorption χ'' decreases with increasing t and is well described by a power-law decay

$$\chi''(t,\omega) = \chi_0''(\omega) + A_0''(\omega)t^{-b''}, \tag{5}$$

where b'' is an exponent, and $\chi_0''(\omega)$ and $A_0''(\omega)$ are t-independent constants. In the limit of $t \to \infty$, $\chi''(t,\omega)$ tends to $\chi_0''(\omega)$. The least-squares fit of the data of $\chi''(t,\omega)$ at T

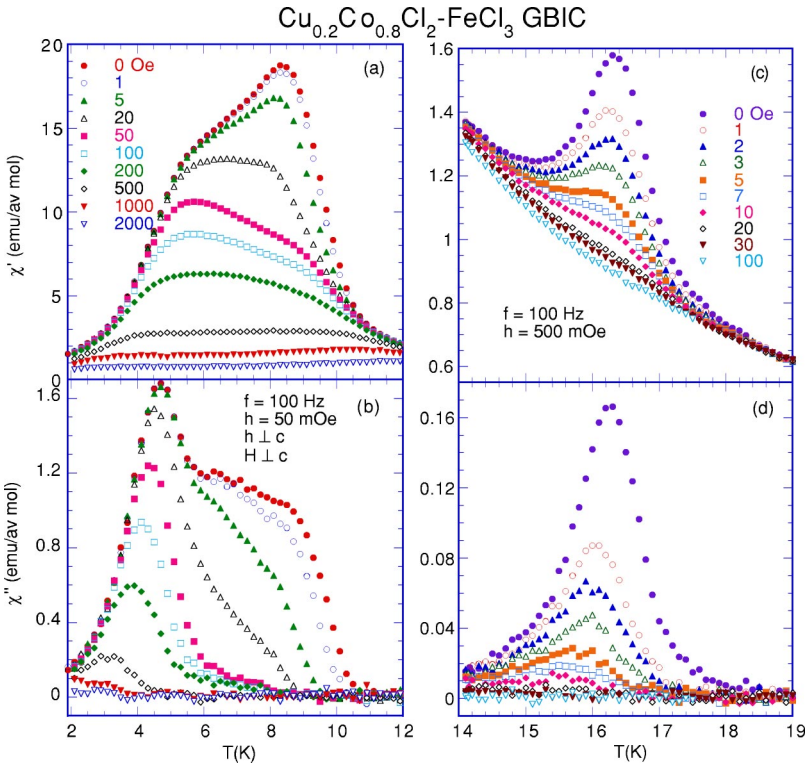

FIG. 10. (Color online) T dependence of (a) χ' and (b) χ'' at various H. H is applied along the c plane perpendicular to the graphene plane ($H\perp c$). $f=100$ Hz, $h=50$ mOe, $h\perp c$, $1.9\leqslant T\leqslant 12$ K. T dependence of (c) χ' and (d) χ'' at various H. $H\perp c$, $f=100$ Hz, $h=500$ mOe, $h\perp c$, $14\leqslant T\leqslant 19$ K.

$=7$ K to Eq. (5) yields parameters listed in Table I. The exponent b'', which is dependent on f, is smaller than that of the FM phase of reentrant ferromagnet[12] $CdCr_{1.8}In_{0.2}S_4$ ($b''\approx 0.2$) and the SG phase of pure spin glass $Fe_{0.5}Mn_{0.5}TiO_3$ ($b''\approx 0.14\pm 0.03$).[35] The value of χ_0'' tends to decrease with increasing f. In contrast, the value of A'' tends to increase with increasing f. It follows that the second term of Eq. (5) cannot be described by a power form $(\omega t)^{-b''}$, suggesting no ωt-scaling law in the form of χ'' $\approx(\omega t)^{-b''}$. This is in contrast to the ωt-scaling of χ'' in the FM phase of reentrant ferromagnet $CdCr_{1.8}In_{0.2}S_4$.[12] The t dependence of χ' can be also described by the power-law form ($\approx t^{-b'}$) which is similar to Eq. (5). The value of b' at $T=7$ and 8.5 K which is listed in Table I is on the same order as that of b''. Note that similar aging behavior is also observed both in χ'' and χ' below T_{RSG}. The change of χ'' and χ' with t below T_{RSG} is not so prominent

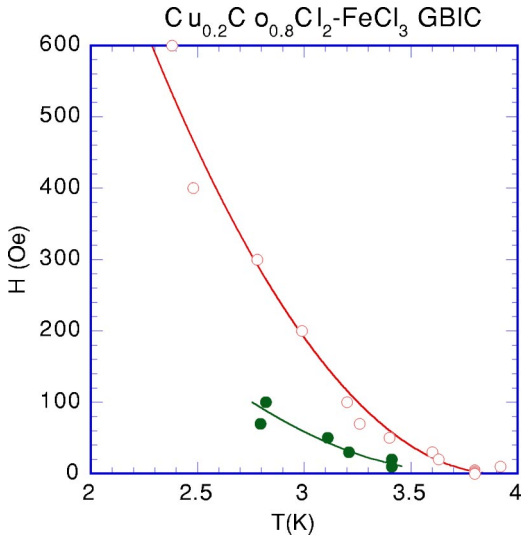

FIG. 11. (Color online) H-T phase diagram near T_{RSG}: for each H the local-minimum temperatures of $d\delta\chi/dT$ vs T (●) and the peak temperature of χ'' vs T at 0.1 Hz (○). The solid lines denote the least-squares-fitting curves (see the text for detail).

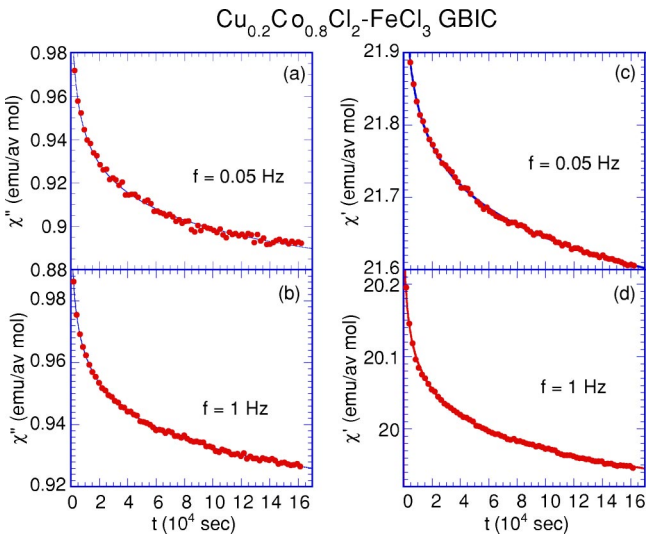

FIG. 12. (Color online) t dependence of (a) and (b) χ'', and (c) and (d) χ' at $T=7$ K for $f=0.05$ and 1 Hz, where t is the time taken after the sample was quenched from 100 K to $T=7$ K. $H=0$. The solid lines denote the least-squares-fitting curves (see the text for detail).

TABLE I. Exponents b'' and b' determined from the least-squares fits of $\chi''(t,\omega)$ and $\chi'(t,\omega)$ at f to the power-law form given by Eq. (5) for $\chi''(t,\omega)$ and the corresponding equation for $\chi'(t,\omega)$. $T=7$ and 8.5 K.

T(K)	f(Hz)	b''	b'
7	0.05	0.074 ± 0.016	
7	0.1	0.045 ± 0.013	0.012 ± 0.005
7	0.5	0.042 ± 0.008	0.045 ± 0.005
7	1	0.029 ± 0.006	0.046 ± 0.006
7	5	0.015 ± 0.025	0.070 ± 0.016
8.5	0.05	0.147 ± 0.067	
8.5	0.5	0.065 ± 0.028	
8.5	1	0.046 ± 0.022	0.038 ± 0.011

compared to that above T_{RSG}, partly because of relatively small magnitude of χ'' and χ' below T_{RSG}.

IV. DISCUSSION

It is interesting to compare the nature of the RSG phase of $Cu_{0.2}Co_{0.8}Cl_2$-$FeCl_3$ GBIC (denoted as $c=0.2$ for simplicity) with that of the SG phase of $Cu_{0.5}Co_{0.5}Cl_2$-$FeCl_3$ GBIC ($c=0.5$).[23,24]

(i) The relaxation time τ for $c=0.5$ is described by Eq. (3) with T_{SG} instead of T_{RSG}, where $T_{SG}=3.92\pm0.11$ K, $x=10.3\pm0.7$, and $\tau^*=(5.27\pm0.07)\times10^{-6}$sec. These values of the dynamic critical exponent x and τ^* are on the same order as those for $c=0.2$ [$x=8.5\pm1.8$ and $\tau^*=(4.77\pm0.10)\times10^{-6}$sec].

(ii) The critical exponent β ($=0.36\pm0.03$) for $c=0.5$ is much smaller than β ($=0.57\pm0.10$) for $c=0.2$.

(iii) The exponents α' and α'' for $c=0.5$ ($\alpha'=0.111\pm0.001$ and $\alpha''=0.096\pm0.003$) are a little larger than those for $c=0.2$ ($\alpha'\approx0.08$–0.09 and $\alpha''\approx0.08$).

(iv) The absorption $\chi''(\omega,t)$ below T_{SG} for $c=0.5$ obeys a $(\omega t)^{-b''}$-scaling law decay with an exponent $b''\approx0.255\pm0.005$. This value of b'' is relatively larger than that for $c=0.2$.

In spite of the difference in detail, it is concluded that the nature of the RSG phase for $c=0.2$ is similar to that of the SG phase for $c=0.5$. This suggests that the RSG phase below T_{RSG} is not a mixed phase but a normal SG phase.

In contrast, the FM phase of our system is very different from that of regular FM phase. The chaotic behavior observed in the FM phase is rather similar to that in the RSG phase. The prominent nonlinear susceptibility of the FM phase arises mainly from the unfrustrated ferromagnetically ordered spins (the FM network). The aging phenomena of $\chi''(t)$ are observed in the FM phase. These results can be well explained in terms of the phenomenological random-field picture proposed by Aeppli *et al.*[6] (see Sec. I). The FM phase consists of the FM network (with slow dynamics) surrounded by frustrated spins (the PM clusters with fast dynamics). Such a nonuniformity gives rise to the chaotic nature of the FM phase. On approaching T_{RSG} from the high-T side, the thermal fluctuations of the spins in the PM clusters become so slow that the slow dynamics of the FM network is significantly influenced by the dynamics of the PM clusters. The coupling between the FM network and the PM clusters becomes important. The molecular fields from the slow PM spins act as a random magnetic field. This causes breakups of the FM network into finite-sized clusters. Below T_{RSG}, the system becomes the RSG phase.

Next we discuss the nature of the aging phenomena in the FM phase. The features of the aging phenomena are summarized as follows.

(i) Both $\chi''(t,\omega)$ and $\chi'(t,\omega)$ at $T=7$ and 8.5 K have power-law forms ($\chi''\approx t^{-b''}$ and $\chi'\approx t^{-b'}$) at fixed f ($=\omega/2\pi$). The values of b' and b'' are listed in Table I.

(ii) $\chi''(\omega)$ for $6.1\leqslant T\leqslant7.3$ K has a power-law form ($\chi''\approx\omega^{\beta''}$), where $\beta''=0.04\pm0.01$ at 6.1 K and 0.12 ± 0.01 at 7.2 K.

The increase of $\chi''(\omega)$ with increasing ω is similar to that reported in conventional SG's such as $Fe_{0.5}Mn_{0.5}TiO_3$.[27] In our system, we find $b''=0.074\pm0.016$ ($T=7$ K and $f=0.05$ Hz), and $b'=0.046\pm0.006$ ($T=7$ K, $f=1$ Hz), and $\beta''=0.081\pm0.02$ ($T=6.7$ K). There are relatively large differences among β'', b', and b'', depending on the conditions. Nevertheless, we can say that these exponents are roughly the same and are on the order of 0.05–0.08 around 7 K. The value of these exponents is nearly equal to that of the exponent $y(=0.066\pm0.001)$ derived from the scaling analysis in Sec. III B. The exponent y is given by $y=\beta/x$, where $x=\nu z$. When we use the scaling relation $\beta=2\nu\theta$, which is derived in our previous paper,[23] y is given by $y=2\theta/z$, where θ is the energy exponent and z is the dynamic critical exponent. The values of θ and z are theoretically predicted: $z=6.0\pm0.5$ for the 3D $\pm J$ Ising spin-glass model (Ogielski[28]) and $\theta=0.19\pm0.01$ (Bray and Moore[36]). Using these values, y is estimated as $y=0.063\pm0.017$, which is in good agreement with our result ($y=0.066\pm0.001$).

V. CONCLUSION

The nonlinear susceptibility and aging phenomena are observed in the FM phase of the reentrant ferromagnet $Cu_{0.2}Co_{0.8}Cl_2$-$FeCl_3$ GBIC. These results indicate that the FM phase between T_{RSG} and T_c has a chaotic nature. The absorption $\chi''(t,\omega)$ is described by a power-law form $t^{-b''}$ but not by a ωt-scaling form $(\omega t)^{-b''}$. Further studies on aging behaviors including memory effect, rejuvenation, and wait time dependence are required to understand the nature of the FM phase, with the same qualitative features as in conventional spin glasses.

ACKNOWLEDGMENTS

We would like to thank H. Suematsu for providing us with single-crystal kish graphite, T.-Y. Huang for his assistance in susceptibility measurements, and T. Shima and B. Olson for their assistance in sample preparation and x-ray characterization. Early work, in particular for the sample preparation, was supported by NSF Grant No. DMR 9201656.

*Email address: suzuki@binghamton.edu
†Email address: itsuko@binghamton.edu

[1] K. Motoya, S.M. Shapiro, and Y. Muraoka, Phys. Rev. B **28**, 6183 (1983).
[2] J. Suzuki, Y. Endoh, M. Arai, M. Furusaka, and H. Yoshizawa, J. Phys. Soc. Jpn. **59**, 718 (1990).
[3] J.A. Geohegan and S.M. Bhagat, J. Magn. Magn. Mater. **25**, 17 (1981).
[4] K. Jonason, J. Mattsson, and P. Nordblad, Phys. Rev. B **53**, 6507 (1996).
[5] K. Jonason, J. Mattsson, and P. Nordblad, Phys. Rev. Lett. **77**, 2562 (1996).
[6] G. Aeppli, S.M. Shapiro, R.J. Birgeneau, and H.S. Chen, Phys. Rev. B **28**, 5160 (1983).
[7] T. Sato, T. Ando, T. Ogawa, S. Morimoto, and A. Ito, Phys. Rev. B **64**, 184432 (2001).
[8] T. Ogawa, H. Nagasaki, and T. Sato, Phys. Rev. B **65**, 024430 (2001).
[9] J.L. Dormann, A. Saifi, V. Cagan, and M. Nogues, Phys. Status Solidi B **131**, 573 (1985).
[10] M. Alba and J. Hammann, J. Magn. Magn. Mater. **54-57**, 213 (1986).
[11] S. Pouget and M. Alba, J. Phys.: Condens. Matter **7**, 4739 (1995).
[12] V. Dupuis, E. Vincent, M. Alba, and J. Hammann, Eur. Phys. J. B **29**, 19 (2002).
[13] H. Maletta, G. Aeppli, and S.M. Shapiro, Phys. Rev. Lett. **48**, 1490 (1982).
[14] G. Aeppli, H. Maletta, S.M. Shapiro, and D. Abernathy, Phys. Rev. B **36**, 3956 (1987).
[15] P. Mathieu, P. Nordblad, D.N.H. Nam, N.X. Phuc, and N.V. Khiem, Phys. Rev. B **63**, 174405 (2001).
[16] D. Sherrington and S. Kirkpatrick, Phys. Rev. Lett. **32**, 1792 (1975).
[17] S.F. Edwards and P.W. Anderson, J. Phys. F: Met. Phys. **5**, 965 (1975).
[18] G. Parisi, Phys. Rev. Lett. **43**, 1754 (1979).
[19] G. Toulouse, J. Phys. (France) Lett. **41**, L447 (1980).
[20] I.S. Suzuki, M. Suzuki, H. Satoh, and T. Enoki, Solid State Commun. **104**, 581 (1997).
[21] I.S. Suzuki, M. Suzuki, H. Satoh, and T. Enoki, Mol. Cryst. Liq. Cryst. **340**, 107 (2000).
[22] M. Suzuki and I.S. Suzuki, Phys. Rev. B **59**, 4221 (1999).
[23] I.S. Suzuki and M. Suzuki, Phys. Rev. B **68**, 094424 (2003).
[24] M. Suzuki and I.S. Suzuki, Eur. Phys. J. B, cond-mat/0308285 (to be published).
[25] M. Suzuki, I.S. Suzuki, and T.-Y. Huang, J. Phys.: Condens. Matter **14**, 5583 (2002).
[26] T. Sato and Y. Miyako, J. Phys. Soc. Jpn. **51**, 1394 (1981).
[27] K. Gunnarsson, P. Svedlindh, P. Nordblad, L. Lundgren, H. Aruga, and A. Ito, Phys. Rev. Lett. **61**, 754 (1988).
[28] A.T. Ogielski, Phys. Rev. B **32**, 7384 (1985).
[29] W. Kleemann, P. Petracic, Ch. Binek, G.N. Kakazei, Yu.G. Pogorelov, J.B. Sousa, C. Cardoso, and P.P. Freitas, Phys. Rev. B **63**, 134423 (2001).
[30] S. Geschwind, D.A. Huse, and G.E. Devlin, Phys. Rev. B **41**, 4854 (1990).
[31] K. Gunnarsson, P. Svedlindh, P. Nordblad, L. Lundgren, H. Aruga, and A. Ito, Phys. Rev. B **43**, 8199 (1991).
[32] W. Adbul-Razzaq, J.S. Kouvel, and H. Claus, Phys. Rev. B **30**, 6480 (1984).
[33] W. Adbul-Razzaq and J.S. Kouvel, Phys. Rev. B **35**, 1764 (1987).
[34] B.K. Srivastava, A. Krishnamurthy, V. Ghose, J. Mattsson, and P. Nordblad, J. Magn. Magn. Mater. **132**, 124 (1994).
[35] V. Dupuis, E. Vincent, J.-P. Bouchaud, J. Hammann, A. Ito, and H. Aruga Katori, Phys. Rev. B **64**, 174204 (2001).
[36] A.J. Bray and M.A. Moore, Phys. Rev. Lett. **58**, 57 (1987).